

## QUASI-PLASTIC CONSTITUTIVE MODEL OF STEEL FIBRE REINFORCED CONCRETE

J. Brauns & K. Rocens

To cite this article: J. Brauns & K. Rocens (1998) QUASI-PLASTIC CONSTITUTIVE MODEL OF STEEL FIBRE REINFORCED CONCRETE, *Statyba*, 4:4, 274-279, DOI: [10.1080/13921525.1998.10531417](https://doi.org/10.1080/13921525.1998.10531417)

To link to this article: <https://doi.org/10.1080/13921525.1998.10531417>



Published online: 26 Jul 2012.



Submit your article to this journal [↗](#)



Article views: 70

---

## QUASI-PLASTIC CONSTITUTIVE MODEL OF STEEL FIBRE REINFORCED CONCRETE

J. Brauns, K. Rocens

### 1. Introduction

Fibre-reinforced cementitious composites are characterized by matrices that are quasi-brittle, by fibres that are relatively ductile, and by interfaces that can transfer important shear forces between the constituents [1,2]. The flexural behaviour of fibre reinforced concrete (FRC) members can be determined during the direct loading. Nevertheless, in the structural design of fibre reinforced elements and for determining the possibility to use the material in a cracked range [3-6], a semi-empirical approach is developed. On the basis of material characteristics in the direct uniaxial tension and compression and spatial arrangement of the reinforcement, mathematical models for prognoses of the material properties in flexure were proposed and tested.

A semi-empirical approach was developed to determine the moment-curvature behaviour of FRC members. The approach was applied assuming a pure bending and using an idealized FRC stress-strain diagram. The degree of anisotropy, ie the reinforcement arrangement in solid concrete was determined by using the stereological principle and electromagnetic method. The analytical predictions showed a good agreement with the experimentally obtained data.

### 2. Experimental procedure

#### 2.1. Specimens

Fibre-reinforced concrete (FRC) specimens with randomly oriented short non-galvanized steel fibres were tested in the uniaxial tension and compression, as well as flexure. Three different fibre volume fractions  $V_f$  were used: 2%, 3%, and 4%. All fibres were 0.3 mm in diameter. Fibre lengths were 35 and 40 mm. Fibres were cut to the desired lengths using a manual table-top cutting machine. Matrix mix proportions

were 1/2.5/0.55 by weight of Portland cement, fine sand, and water, respectively. Modulus of the wire was 210 GPa and the yield strength was about 1.2 GPa. Wire surfaces were cleaned by acetone to remove the oil.

Sand and cement were first mixed with a rotary-type mixer. After the wet mixture had attained a uniform consistency, fibres were added slowly to prevent bundling and to ensure a random distribution. Wet mixing of the materials was done for about 3 min. The specimens were cast into properly oiled steel forms. In order to obtain a uniform compacting the vibration time was for 1 min. The specimens were demolded 24 h after the casting and were cured in a humid room. The specimens were capped before allowed to dry for 2 days and were tested at the age of 2 months.

#### 2.2. Tension tests

In the direct tension the tests with eight-form specimens with cross-section 5x5 cm were used. The specimens failed at the weak section soon after the cracking of the mortar. Typical tensile stress-strain curves are shown in Fig 1.

The specimens exhibited almost entirely linear behaviour up to the cracking stress of 3.0-3.5 MPa, after which a load drop-off was observed. Tensile strains were calculated from the measured displacements obtained by using the linear variable differential transformer (LVDT) with a gauge length of 70 mm.

#### 2.3. Axial compression tests

The compression specimens were prismatic 7x7x28 cm. The tests in the uniaxial compression showed that the transition from the linear elastic behaviour to the non-linear was a smooth one. At ultimate

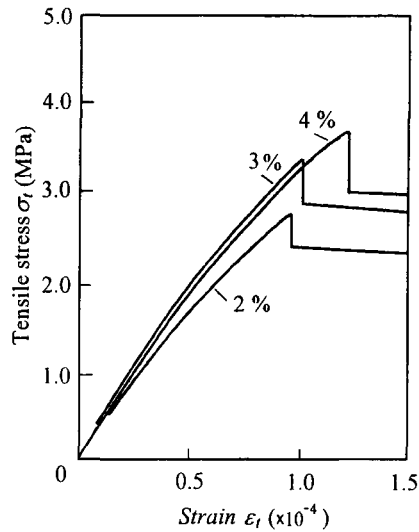


**Fig 1.** Typical tensile stress-strain diagrams of reinforced concrete with fibre volume fraction  $V_f$  (%)

ultimate condition the fibres would tend to buckle, causing premature spalling of the mortar. The failure occurred at the stress level of 35-40 MPa

#### 2.4. Bending tests

The flexure specimens (5x5x54 cm) were simply supported and subjected to the third-point loading. The extreme fibre strains at mid-span and central deflections were measured by LVDT and dial gauges, respectively. Because non-linear character of the load-deflection relationships was initiated by the cracking of the matrix, the appearance of the cracks in the middle third of the span was observed carefully during the test. First cracks were visible by the naked eye only when the load was nearing its ultimate value, and the cracks widened until failure. No crushing in the compression zone of the specimens was observed up to the collapse.

#### 2.5. Estimation of fibre orientation

The orientation of steel fibre is generally influenced by such factors as the direction of casting, method of compacting, size of specimen, size and volume fraction of steel fibre, and mix proportions of the matrix concrete [7-9].

The stereological approach [10] was used for the determination of the structural anisotropy of a composite. After mechanical testing cubes (4.5x4.5x4.5

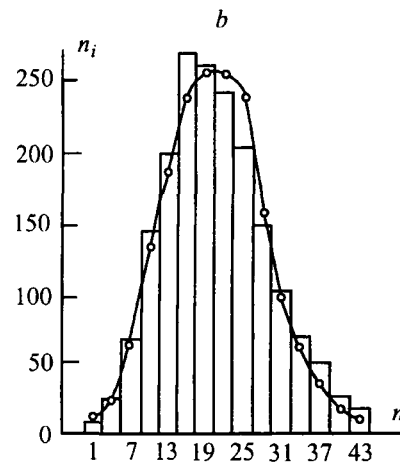
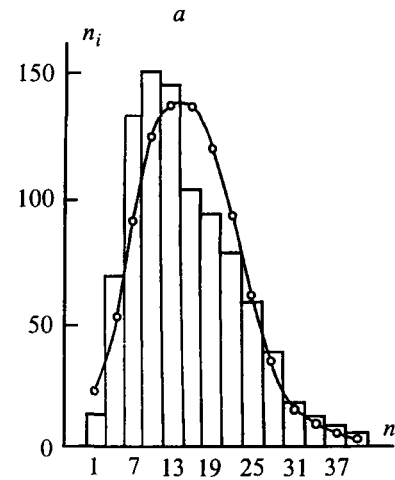


**Fig 2.** Histograms of fibre intersection numbers  $n$  per unit area ( $V_f = 2\%$ ) and Gauss distribution curves: (a) horizontal planes, (b) vertical planes

cm) from the specimens were cut out. On new surfaces the number of fibre intersections per unit area for each different orientation of the cutting plane was counted. These observed data were related to the distribution density of fibres and characterized the internal structure of the composite. The measurement of such density was impractical, and in many cases impossible. The stereological procedure gave an indirect way of the estimation of that density.

In order to determine the degree of technological anisotropy, horizontal ( $xz$ ) and vertical ( $xy$  and  $yz$ ) planes of reinforced concrete cubes were examined. For volume fraction of steel fibre, eg  $V_f = 2\%$ , the mean values of fibre intersections were  $n_{xz} = 19.9$ ,  $n_{yz} = 20.9$ ,  $n_{xy} = 14.2$  and standard deviations 7.03,

7.62, 7.18, respectively. In Fig 2 histograms showing the distribution of fibre intersection numbers  $n_i$  with the number per unit area  $n$  and theoretical distribution curves depending on the plane orientation are given. On the basis of statistical estimation it was concluded that the mean values were equal in vertical planes and differed from those in a horizontal plane. Also the ferromagnetic method was applied. The ratio of relative indices in the horizontal and vertical directions was about 3:2.

### 3. Theoretical considerations

#### 3.1. Flexural behaviour of fibre reinforced concrete

Because plates and shells are the most widely distributed fields of the application of fibre reinforced concrete [11-13], the problem to find the strains of such elements is associated with the variation of stiffness dependent on the deformation process. In this study even in the uncracked range, the element in bending was treated as a two-layered system [14,15]. For the initial stage of deformation, different moduli in tension and compression were taken into account. In the cracked range the action of quasi-plastic tensile material behaviour was modeled by using an idealized stress-strain diagram, as shown in Fig 3.

The stress distribution had different modes depending on the progress of loading. At low load levels, the stress distribution was represented by a straight line with the neutral axis at beam centre. With the further load increase, beyond the cracking strength of a composite material, the stress distribution in the tensile zone would acquire radical changes and as a limit approached a constant value, as shown in the

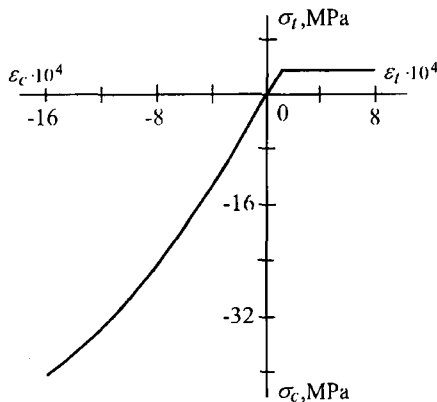


Fig 3. Idealized stress-strain diagram ( $V_f = 2\%$ )

idealized stress distribution diagram. The resistance and debonding behaviour as well as the orientation of fibres accounted for the action of quasi-plastic tensile stresses. Of course, these stresses were not the actual properties because they were determined by the mean values of fibre forces per unit area.

#### 3.2. Mathematical approach

In the analysis, it was assumed that the rectangular cross-section of fibre reinforced beams was symmetrical about the  $y$  axis and that the plane in which the bending moment acted passed through the axis of symmetry (Fig 4). According to the loading scheme the middle third of the element was under a pure bending. Let the distance between the neutral axis  $x_0$  and axis of gravity  $x_c$  be  $e$ , and the depth of beam  $h = h_A + h_B$ . At any distance  $y$  from the neutral axis the strain was

$$\varepsilon(y) = \frac{y+e}{R}, \quad (1)$$

where  $R$  is the radius of curvature.

The tensile strain in the outermost fibre was

$$\varepsilon_t = \frac{h_A + e}{R} \quad (2)$$

and the compressive strain was

$$\varepsilon_c = \frac{h_B - e}{R}. \quad (3)$$

From Eqs (2) and (3) the curvature would be

$$\kappa = \frac{1}{R} = \frac{\varepsilon_t - \varepsilon_c}{h}. \quad (4)$$

Considering the section shown, for equilibrium the resultant of the normal stresses vanished [16], that was

$$\int_{h_B}^{h_A} \sigma b dy = 0. \quad (5)$$

Combining Eqs (1) to (5) lead to

$$\int_{\varepsilon_c}^{\varepsilon_t} \sigma b d\varepsilon = 0. \quad (6)$$

By applying the Eqs (1) to (6) and assuming the pure bending, according to the hypothesis of flat sections, the bending moment was given by

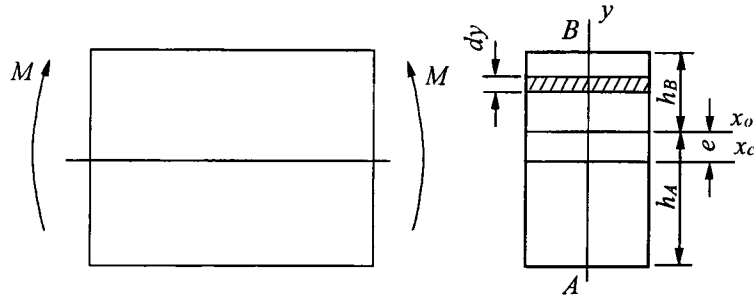


Fig 4. Element of beam in bending and cross-section with axes

$$M = \frac{bh^2}{(\epsilon_t - \epsilon_c)} \int_{\epsilon_c}^{\epsilon_t} \sigma \epsilon d\epsilon. \quad (7)$$

Basing on the expressions for the area  $\sigma$ - $\epsilon$  and static moment of this area, in the equilibrium state we had

$$\Phi(\epsilon_t) = \Phi(\epsilon_c) \quad (8)$$

$$M = \frac{bh^2}{(\epsilon_t - \epsilon_c)^2} [\Psi(\epsilon_t) - \Psi(\epsilon_c)] \quad (9)$$

where  $\Phi$  and  $\Psi$  were the functions of  $\sigma$ - $\epsilon$  diagram area and static moment of this area, respectively. Fig 5 shows the semi-empirical solution for  $\epsilon_c$ ,  $\Psi(\epsilon_t)$  and  $\Psi(\epsilon_c)$  at given  $\epsilon_t$

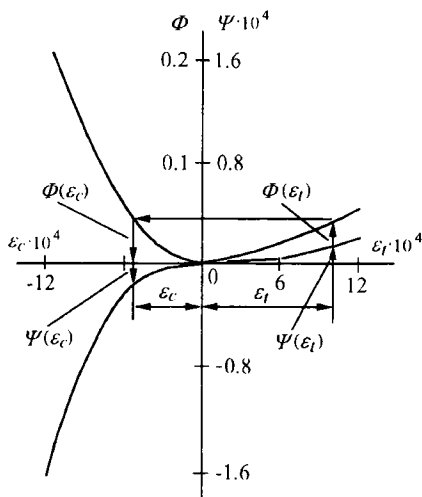


Fig 5. Plots of functions  $\Phi$  and  $\Psi$  ( $V_f = 2\%$ )

#### 4. Numerical results and discussion

According to the equations (4), (9) and Fig 4, theoretical values of curvature  $\kappa$  versus the bending moment of the bent fibre reinforced elements were predicted (Fig 6); ie on the basis of the material properties in the direct uniaxial loading the relation moment-curvature was determined. By using the deformations  $\epsilon_t$ ,  $\epsilon_c$  and the deflection  $w$  the experimental values of the curvature were found. The curvature with the deflection was given by the expression

$$\kappa(M) = \frac{w(M)}{s l^2}, \quad (10)$$

where  $l$ ,  $s$  were the span of simply supported beam and coefficient for the given loading scheme, respectively. In Fig 6 the curves 2 and 3 show the average deformability of 6 beams. The curves 4 and 5 are plotted for the beams with the highest flexural deformability. It is seen that the theoretical bending curve is below (10-15%) the average one.

On the basis of the theoretical bending curve (solid line 1, Fig 6), the variation of stiffness  $D$  with the bending moment was fixed. The comparison between the analytical and experimental values of stiffness of fibre reinforced beams is shown in Fig 7. The experimental values of stiffness with the bending moment were defined by using the experimental value of strains of outermost fibres

$$D_\epsilon(M) = \frac{M}{\epsilon_t - \epsilon_c}. \quad (11)$$

Similarly, on the basis of the deflections the stiffness was found

$$D_w(M) = \frac{s M l^2}{w}. \quad (12)$$

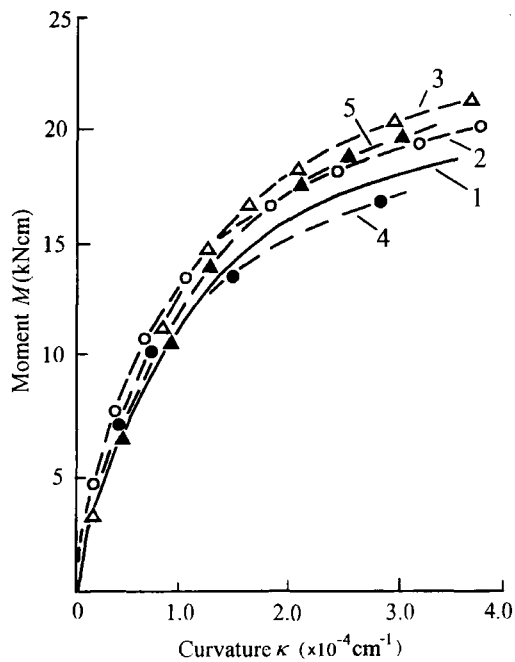


Fig 6. Theoretical (1) and experimental (2-5) bending curves of reinforced beams ( $V_f = 2\%$ ): 2,4 -  $\kappa(\epsilon)$ ; 3,5 -  $\kappa(w)$

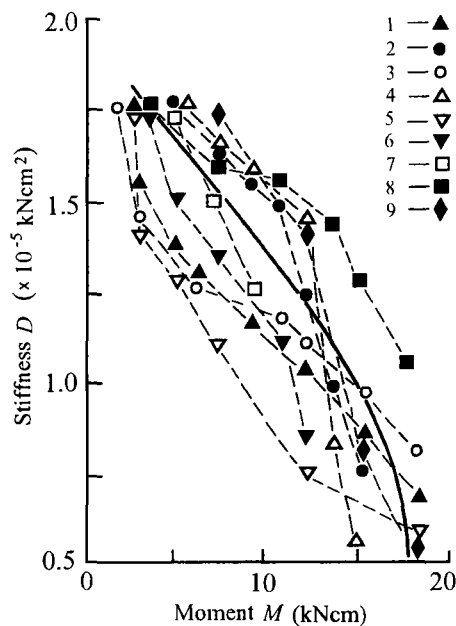


Fig 7. Dependencies of stiffness of reinforced elements on the bending moment: solid line - predicted curve; experimental dots: 1 -  $D_w$ ;  $d_f = 0.3$  mm,  $l_f = 25$  mm,  $V_f = 3\%$ ; 2 -  $D_e$ ; 0.3, 25, 3; 3 -  $D_w$ ; 0.3, 25, 4; 4 -  $D_e$ ; 0.5, 25, 2; 5 -  $D_w$ ; 0.5, 30, 3; 6 -  $D_w$ ; 0.5, 30, 2; 7 -  $D_w$ ; 0.5, 35, 2; 8 -  $D_e$ ; 0.4, 30, 3; 9 -  $D_e$ ; 0.5, 30, 3

As seen in Fig 7, the stiffnesses determined by using strains  $\epsilon_c$  and  $\epsilon_t$  are above those found by the deflections. The experimental dots show the average values of 5 or 6 samples.

## 5. Conclusions

On the basis of the experimentally determined properties of FRC in the uniaxial compression and tension, a semi-empirical method for the estimation of moment-curvature behaviour of FRC members was developed. The reinforced elements as a two-layered system were treated and in the cracked range the action of quasi-plastic tensile stresses by using the idealized stress-strain diagram was considered. The properties of reinforced concrete in the compression, tension and bending for the specimens with certain structural anisotropy were determined. Principally the fibres were oriented in the direction of stress, ie perpendicularly to the casting direction. For the estimation of the degree of technological anisotropy the stereological principles by counting the number of fibre intersections per unit area for each different orientation as well as the ferromagnetic method were used.

## References

1. Y. Shao, Z. Li, S. P. Shah. Matrix cracking and interface debonding in fiber-reinforced cement-matrix composites // *Advn. Cem. Bas. Mat.*, 1, 1993, p. 55-66.
2. S. P. Shah, C. Ouyang. Mechanical behaviour of fiber-reinforced cement-based composites // *J. Am. Ceram. Soc.*, 74, 1991, p. 2727-2738.
3. J. P. Romualdi, G.B. Batson. Behaviour of reinforced concrete beams with closely spaced reinforcement // *ACI Journal Proceedings*, 60, 1963, p. 775-789.
4. S. P. Shah, B. V. Rangan. Fiber reinforced concrete properties // *ACI Journal Proceedings*, 68, 1971, p. 126-135.
5. J. Brauns. Quasi-plastic deformation and strength of fibre reinforced concrete structures // *Mech. of Comp. Mater.*, 30, 1994, p. 675-679.
6. D. J. Hannat. The effect of post cracking ductility on the flexural strength of fiber cement and concrete // *RILEM Symposium "Fiber Reinforced Cement and Concrete"*, England: Construction Press, 1975, p. 499-508.
7. B. Maidl. *Stahlfaserbeton*. Berlin: Ernst & Sohn, 1991, 366 S.
8. J. Brauns, K. Rocens. Effect of reinforcement structure on deformation and strength of steel fibre concrete // *Proceedings of 4<sup>th</sup> International Conference "Modern Building Materials, Structures and Techniques"*, Vilnius, Lithuania: Technica, 1995, p. 25-30.

9. Y. Tanigawa, K. Yamada, S. Hatanaka, H. Mori. A simple constitutive model of steel fibre reinforced concrete // *Int. J. Cem. Comp. Light. Concr.*, 5, 1983, p. 87-96.
10. K. Kanatani. Stereological determination of structural anisotropy // *Int. J. Engng. Sci.*, 22, 1984, p. 531-546.
11. R. N. Swamy. Properties and Applications of Fibre Reinforced Concrete, Paper 1-3, Otaniemi. Finland, 1974, 82 p.
12. R. F. Zollo. Wire fiber reinforced concrete overlays for orthotropic bridge deck type loadings // *ACI Journal Proceedings*, 72, 1975, p. 576-582.
13. T. Y. Lim, P. Paramasivam, S. L. Lee. Bending behaviour of steel-fiber concrete beams // *ACI Structural Journal*, 1987, 84, p. 524-536.
14. M. A. Ghalib. Moment capacity of steel fiber reinforced small concrete slabs // *ACI Journal*, 77, 1980, p. 247-257.
15. B. Pakotiprapha, R. P. Pama, S. L. Lee. Mechanical properties of cement mortar with randomly oriented short steel wires // *Magazine of Concrete Research*, 26, 1974, p. 3-15.
16. F. H. Faupel, F. E. Fisher. Engineering Design: A Synthesis of Stress Analysis and Materials Engineering. New York: John Wiley & Sons, 1991, 1056 p.

Įteikta 1998 07 02

## KVAZIPLASTINIS KONSTRUKCINIS PLIENFIBRIO BETONO MODELIS

J. Brauns, K. Rocens

### S a n t r a u k a

Buvo sukurtas pusiau empirinis metodas plienfibrio betono elementų darbui nustatyti. Jis grindžiamas tų elementų vienašio tempimo ir gniuždymo bandymais. Metodas buvo plėtojamas remiantis grynuoju lenkimu ir naudojant idealizuotą plienfibrio betono įtempių ir deformacijų diagramą. Taikant stereologinį principą ir elektromagnetinį metodą, buvo nustatomas filtrų pasiskirstymo kietame betone laipsnis. Analitinė prognozė parodė, jog tas laipsnis sutampa su duomenimis, kurie gauti bandymais.

---

**Janis BRAUNS.** Doctor Habil, Associate Professor. Dept of Structural Engineering. Riga Technical University, 16 Azenes St., LV-1048, Riga, Latvia.

A graduate of Riga Technical University (1970). Dr degree in solid mechanics (1974), Dr Habil degree in technological mechanics of composite materials (1995). Research interests: analysis and design of composite materials and composite structures, estimation of environmental effects on composite materials.

---

**Karlis ROCENS.** Doctor Habil, Professor. Head of the Dept of Structural Engineering. Riga Technical University, 16 Azenes St., LV-1048, Riga, Latvia.

A graduate of Riga Technical University (1963). Dr degree in mechanics of composite materials (1968), Dr Habil degree in structural mechanics (1980). Research interests: materials and structural engineering.